Mechanism of Low Schottky Barrier Formation for Chromium/CdZnTe Contact

ARTICLE *in* THE JOURNAL OF PHYSICAL CHEMISTRY C · FEBRUARY 2014

Impact Factor: 4.77 · DOI: 10.1021/jp410780n

THE JOURNAL OF PHYSICAL CHEMISTRY C

Article

pubs.acs.org/JPCC

Mechanism of Low Schottky Barrier Formation for Chromium/CdZnTe Contact

Shouzhi Xi,[†] Wanqi Jie,*[,†] Gangqiang Zha,*[,†] Wenhua Zhang,[‡] Junfa Zhu,[‡] Xuxu Bai,[§] Tao Feng,[†] Ning Wang,[†] Fan Yang,[†] and Rui Yang[†]

[†]State Key Laboratory of Solidification Processing, Northwestern Polytechnical University, Xi'an 710072, People's Republic of China

[‡]National Synchrotron Radiation Laboratory, University of Science and Technology of China, Hefei 230029, People's Republic of China

[§]Key Laboratory of Artificial Structures and Quantum Control (Ministry of Education), Department of Physics, Shanghai Jiao Tong University, Shanghai 200240, People's Republic of China

ABSTRACT: Low Schottky barrier electrode has great significance on CdZnTe semiconductor nuclear radiation detectors. In this work, synchrotron radiation photoemission spectroscopy (SRPES) has been used to study the interface electronic structure of chromium (Cr) and CdZnTe with Cr coverage thicknesses ranging from 6 to 45.7 Å. Interface reaction and diffusion happen during the Cr deposition. A new interface structure CdZnTe−Cr−Te hence forms, which causes a positive dipole layer at the interface. Schottky barrier height (SBH) is reduced by 0.34 eV due to the dipole layer. Cr/CdZnTe interface structure can effectively change the SBH. Therefore, Cr can be a favorable low Schottky barrier electrode material for CdZnTe detector.

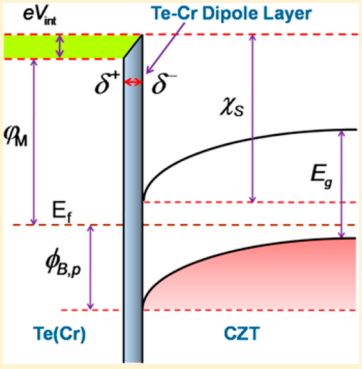

INTRODUCTION

The II−VI compound semiconductor cadmium zinc telluride (CdZnTe or CZT) as an ideal room temperature nuclear radiation detector material has attracted much attention in different important fields, such as nuclear safety inspection, medical imaging, and cosmic radiation detection.[1−5] In addition to the quality of CZT crystal, the metal electrode plays an important role for the detector performance. The contact of metal−semiconductor with good electrical properties[6,7] and adhesion strength[8,9] is the basis for detector fabrication. Schottky barrier height (SBH) has great influence on the electrical properties. Low SBH or even Ohmic contact is of vital importance for semiconductor detectors.[10] However, due to the large work function of p type CZT,[11] it is difficult to find a proper metal to form a low SBH electrode.[11] The common electrode for CZT detector is Au,[12,13] but the poor adhesion of Au on CZT surface limits the detector properties.[8,14] Therefore, it is very meaningful to find a proper electrode material, which will not only form a low SBH contact, but also enhance the interface adhesion with CZT crystal. Cr as a transition metal with one outer electron and highly oriented d orbital can enhance the adhesion strength of Cr−semiconductor contact through interface reaction.[12,15] Therefore it has been widely used for contact material in the semiconductor industry.[16−18] However, the work function of Cr is relatively low, and theoretically it cannot form an Ohmic contact with CZT. Thus, little attempt has been made to fabricate the Cr electrode for CZT detectors. According to former research,[19−21] interface reaction and interdiffusion have significant effects on SBH, especially for a reactive metal like Cr and strong iconicity II−VI semiconductor like CZT.[22,23] So it offers a possibility for Cr to be used as a proper electrode material for CZT detectors.

In this paper, synchrotron radiation photoemission spectroscopy (SRPES) was used to investigate the structural evolution of Cr−CZT interface at room temperature from submonolayer to multilayer of Cr coverage. Interface reaction and interdiffusion process at the interface will be analyzed and the dipole theory will be used to explain the change of SBH. It is expected to establish a deep understanding of the relationship between interface structure and SBH at Cr/CZT interface.

EXPERIMENTAL SECTION

The CZT ingot grown by the Bridgman method in our laboratory[24] was cut into wafers of 9 × 9 × 2 mm^3. The tentative resistivity is 10^{10} Ω cm, and the conductivity is p-type. CZT samples were first mechanically polished by using 0.5 μm size magnesia suspensions and Ludox, and then chemically polished with 2% Br−MeOH solution for 5 min. Afterward, they were rinsed in deionized water and finally dried with nitrogen.

Received: November 1, 2013
Revised: February 17, 2014
Published: February 20, 2014

   dx.doi.org/10.1021/jp410780n | J. Phys. Chem. C 2014, 118, 5294−5298

The experiments of SRPES were carried out at the Surface Physics Station of the National Synchrotron Radiation Laboratory (NSRL) of China in Hefei. The vacuum of the MBE deposition chamber and the analysis chamber is better than 10^{-9} and 10^{-10} Torr, respectively. The analysis chamber is equipped with a VG ARUPS10 electron energy analyzer for SRPES and XPS, a twin-anode X-ray gun, and an Ar^+ sputter gun. The energy resolution ($\Delta E/E$) is better than 10^{-3}.

The clean CZT crystal was kept in the UHV MBE chamber for subsequent Cr growth. To dislodge oxygen and other impurity atoms adsorbed on CZT surface before deposition, the samples was etched for 20 and 10 min by Ar^+ with ionization voltages of 2.0 and 1.0 kV successively, followed by annealing in situ in a vacuum preparation chamber for 10 min. The cleanliness was proved by XPS spectra, and neither C 1s nor O 1s peaks were found. Full-spectrum Cd4d and Te 4d photoemission spectra were taken with the photon energy of 120 eV. The valence band spectra were taken with the photon energy of 28 eV.

RESULTS AND DISCUSSION

The Cd4d, Te4d and Cr3p photoemission spectra of Cr on CZT surface are shown in Figure 1, where all the curves are

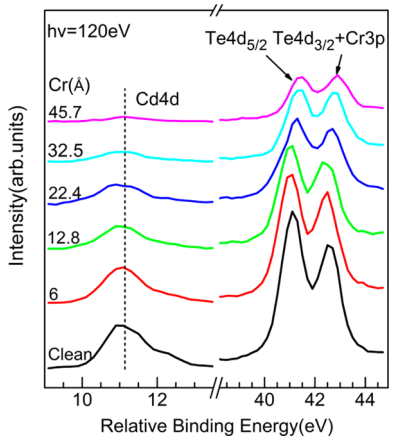

Figure 1. Te4d, Cd4d, and Cr3p core levels and the valence band of Cr/CZT interfaces for various Cr layer thicknesses, recorded at normal emission with photon energy of 120 eV.

normalized. The double peaks at the right side should be composed of $Te4d^{3/2}$, $Te4d^{5/2}$, and Cr3p. Due to the closing peak position of Te4d and Cr3p,[25] the peaks are deconvoluted as shown in Figure 2. According to the evolution of the position and shape of overall peaks, it can be found there are two types of Te atoms with different chemical states. One is combined state Te atoms, and another is reacted state Te atoms. Their Te4d core levels can be defined as Te^c4d and Te^r4d, respectively. The results are similar with the previous observation for the Cr/HgCdTe system.[26−28] As can be seen from Figure 2, the initial peak position of Te^c4d is equal to the binding energy of Te in bulk CZT, and almost stays as a constant in the whole Cr coverage range. The binding energy of Te^r4d starts with 0.85 eV lower than that of Te^c4d at the initial stage of Cr coverage, simultaneously the peak of Cr3p exists with higher binding energy than that of metallic state Cr, which indicates the charge transfer in the chemical reaction between Te and Cr. Beyond 6 Å of Cr layer thickness, the binding energy of Te^r4d increases until the Cr coverage is 22.4 Å, and a

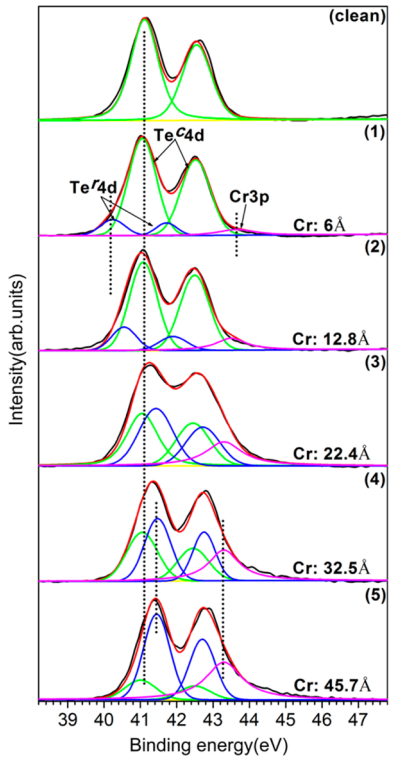

Figure 2. The evolution of Te^c4d, Te^r4d, and Cr3p core levels of Cr/CZT interfaces for various Cr layer thicknesses, recorded at normal emission with photon energy of 120 eV. Black line: experiment results. Red line: results of the best fit.

value of 0.9 eV is reached, meanwhile Cr3p moves toward the lower binding energy by about 0.25 eV; the Te−Cr bond breaking should be responsible for the shift of Te4d and Cr3p, and reflects Te dissociated state and Cr metallic state appearing at the interface after this period of Cr deposition. After 32.5 Å of Cr coverage, the binding energy of Te4d and Cr3p almost stay as a constant, which illustrates the stable states of Te and Cr are formed.

By calculating the peak area of Cd4d, Te4d, and Cr3p core levels, the contents of Cd4d, Te4d, and Cr3p with various Cr coverage are obtained, as shown in Figure 3. It is found that the contents of Cd4d and Te4d decrease with increasing Cr layer thickness. However, the attenuation of Cd4d core level is far more rapid than Te4d, and the content of Te4d is much larger

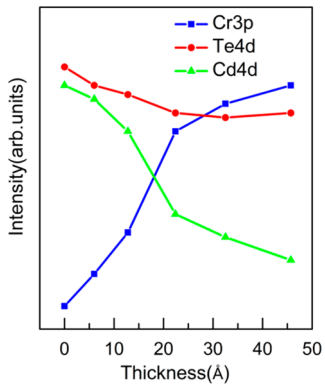

Figure 3. The evolution of Cd4d, Te4d, and Cr3p contents at Cr/CZT interfaces for various Cr layer thicknesses.

dx.doi.org/10.1021/jp410780n | J. Phys. Chem. C 2014, 118, 5294−5298

than Cd4d with Cr layer thickness of 45.7 Å, which indicates Te atoms diffuse to the surface.[28] The evolution of Te^{c}4d and Te^{r}4d contents for various Cr coverage is shown in Figure 4. At

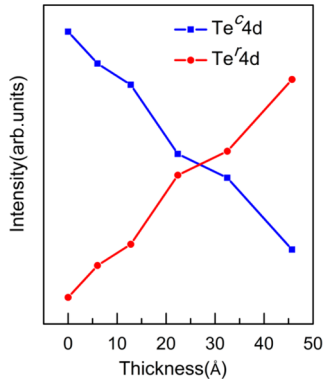

Figure 4. The evolution of Te^{c}4d and Te^{r}4d contents at Cr/CZT interfaces for various Cr layer thicknesses.

low coverage of Cr, the emission spectra are dominated by the intensity of Te^{c}4d, while Te^{r}4d and Cr3p are relatively weak. With increasing Cr layer thickness, Te^{r}4d becomes stronger and finally dominates the spectra. Adding to the evolution of Te^{r}4d binding energy, it is can be concluded that Te^r atoms react with Cr at the initial Cr coverage, then the Te−Cr bond breaking happens as Cr sustained deposition and Te^r component are released from the interface and diffuse to the surface.

The evolution of the valence-band SRPES spectrum with Cr deposition is taken with the photon energy of 28 eV, as shown in Figure 5. All of these spectra are normalized. A clear

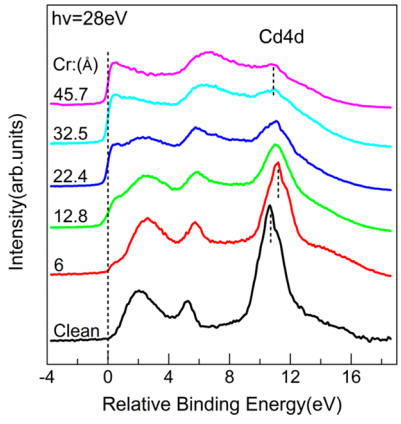

Figure 5. The evolution of valence band at the Cr/CZT interfaces for various Cr layer thicknesses, recorded at normal emission with photon energy of 28 eV.

emission of metallic Fermi edge can be detected at Cr coverage as low as 6 Å, which conforms to the formation of Cr−Te metallic compounds at the surface.[28,29] All Fermi levels are unified and fixed with the relative binding energy of 0 eV. The Cd4d core level first moves to the higher binding energy at a value of 0.5 eV, then decreases gradually to the lower binding energy of 0.34 eV. Since no other peak occurs, the energy shifts should be induced by the change of SBH. Thus, the SBH can be calculated by the value of the core level and the valence band maximum, using the equation[19]

$$\phi_{B,p} = |E_B| - E_{V-C} \quad (1)$$

where $\phi_{B,p}$ is SBH of the metal−semiconductor interface, E_B is the binding energy of the core level, and E_{V-C} is the distance between the core level and the valence band maximum.

The SBH with the function of Cr coverage is shown in Figure 6. A value of 0.82 eV is reached when the thickness of Cr is 6 Å,

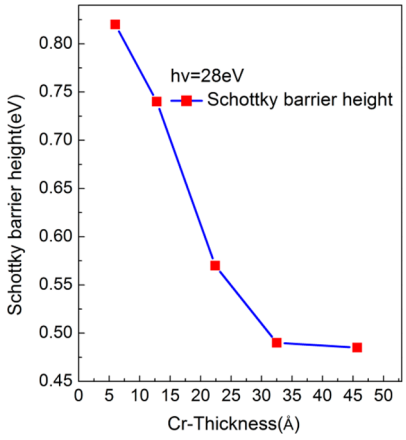

Figure 6. Schottky barrier height decreases for various Cr layer thicknesses.

then it deceases gradually and finally becomes stable with the height of 0.48 eV. The large SBH formed at first for the smaller work function of Cr than that of CZT.[30,31] The Pauling electronegativity of Te is 2.12 eV, larger than that of Cr (1.66 eV). Therefore Cr deposition will lead to a dipole moment, which can be a force driving Te diffusing outward and to the surface. Finally, the interface structure is altered from CZT−Cr to CZT−Cr−Te, which results in an electrical field pointing from Te (δ+) toward CZT/Cr (δ−), and a positive dipole layer at the interface, which should be responsible for the decrease of SBH.[13,32] An energy band alignment of the metal−semi-

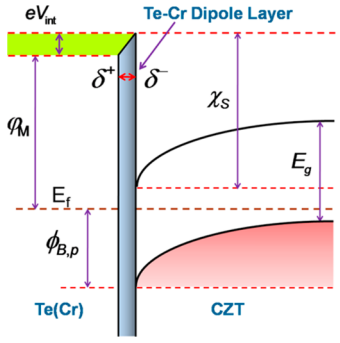

Figure 7. The energy band alignment of the Cr−CZT interface with the Te−Cr dipole layer.

conductor interface with a dipole layer is shown in Figure 7. The SBH to a p-type semiconductor, $\phi_{B,p}$, can be written as[32]

$$\phi_{B,p} = E_g + (\chi_s - \varphi_M) - eV_{int} \quad (2)$$

where φ_M is the work function of Cr, χ_s is the electron affinity of CZT, and V_{int} is the voltage drop at the interface dipole layer. As can be seen from eq 2, first, the $\phi_{B,p}$ decreases as the dipole moment strengthens caused by Te out diffusion, then beyond 32.5 Å, the $\phi_{B,p}$ tends to be a constant as the dipole moment becomes invariable caused by Te−Cr dipole layer formation.

dx.doi.org/10.1021/jp410780n | J. Phys. Chem. C 2014, 118, 5294−5298

To find a more fundamental understanding of the role of Te out diffusion in the dipole layer formation, the surface work functions with various Cr coverage are measured, as shown in Figure 8. The surface work function of clean CZT is measured

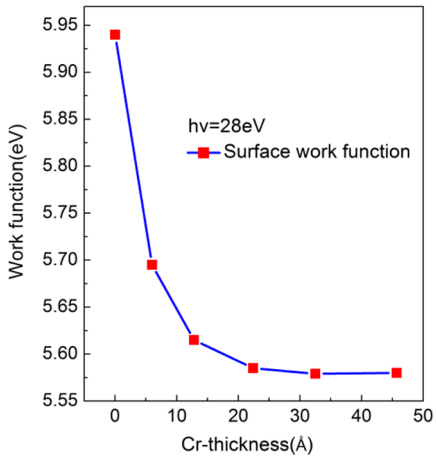

Figure 8. The work function decreases of CZT for various Cr layer thicknesses.

to be 5.94 eV and subsequently the value shows a drop with the Cr deposition, and remains at a constant of 5.58 eV. The final value is about 1.28 eV larger than that of Cr, and should not be caused by the Cr atoms at the surface. The surface work function reduction can be ascribed to the Te−Cr dipole layer.[33,34] With an increase of the Cr layer thickness, the dipole moment is strengthened and drives more Te atoms to move to the surface. Electrons thus move into the surface dipole field and decrease the potential energy when crossing the surface dipole on their way out of the CZT/Cr interface,[35] which decreases the surface work function. Above 32.5 Å, the work function tends to be a constant, which is in accordance with CZT−Cr−Te stable interface structure formation. Apparently, the reduction of the work function is a benefit for Cr to form a low SBH contact with CZT.

CONCLUSIONS

In summary, the electronic properties of the Cr/CZT interface have been studied by synchrotron radiation photoemission measurements. During the deposition of Cr, the Te−Cr chemical reaction first happens and Te atoms are released out from the Cr/CZT interface and diffuse to the surface. The diffusion of elemental Te leads to a new interface structure CZT−Cr−Te, which forms a positive dipole layer pointing from Te ($\delta+$) toward the CZT/Cr ($\delta-$) at the Cr/CZT interface. The SBH reduction from 0.82 eV to 0.48 eV is caused by the formation of this interface dipole layer related to Cr deposition. Thus Cr is proved to be a proper electrode to form a favorable contact with relatively low SBH for CZT semiconductor detectors. The good adhesive offers a better prospect to fabricate Cr/CZT/Cr detectors.

AUTHOR INFORMATION

Corresponding Authors

*E-mail: (W.J.) jwq@nwpu.edu.cn.
*E-mail: (G.Z.) zha_gq@nwpu.edu.cn.

Notes

The authors declare no competing financial interest.

ACKNOWLEDGMENTS

This work has been supported by the Special Fund of National Key Scientific Instrument and Equipment Development (2011YQ040082), the National 973 Project of China (2011CB610400), the 111 Project of China (B08040), and the National Natural Science Foundation of China (50902113, 50902114). The project was also supported by the fund of the State Key Laboratory of Solidification Processing in NWPU (SKLSP201219). The authors are grateful to all of the members of NSRL for their help with the experiments.

REFERENCES

(1) Yin, Y.; Chen, X.; Wu, H.; Komarov, S.; Garson, A.; Li, Q.; Guo, Q.; Krawczynski, H.; Meng, L.-J.; Tai, Y.-C. 3-D Spatial Resolution of 350 mum Pitch Pixelated CdZnTe Detectors for Imaging Applications. *IEEE Trans. Nucl. Sci.* **2013**, *60*, 9−15.

(2) Nelson, K. A.; Geuther, J. A.; Neihart, J. L.; Riedel, T. A.; Rojeski, R. A.; Ugorowski, P. B.; McGregor, D. S. Nuclear Reactor Pulse Tracing Using a CdZnTe Electro-optic Radiation Detector. *Nucl. Instrum. Methods Phys. Res., Sect. A* **2012**, *680*, 97−102.

(3) Komarov, S.; Yin, Y. Z.; Wu, H. Y.; Wen, J.; Krawczynski, H.; Meng, L. J.; Tai, Y. C. Investigation of the Limitations of the Highly Pixilated CdZnTe Detector for PET Applications. *Phys. Med. Biol.* **2012**, *57*, 7355−7380.

(4) Li, Q.; Beilicke, M.; Lee, K.; Garson, A., III; Guo, Q.; Martin, J.; Yin, Y.; Dowkontt, P.; De Geronimo, G.; Jung, I.; Krawczynski, H. Study of Thick CZT Detectors for X-ray and Gamma-ray Astronomy. *Astropart. Phys.* **2011**, *34*, 769−777.

(5) Sellin, P. J. Recent Advances in Compound Semiconductor Radiation Detectors. *Nucl. Instrum. Methods Phys. Res., Sect. A* **2003**, *513*, 332−339.

(6) Wolf, H.; Kronenberg, J.; Wagner, F.; Deicher, M.; Wichert, T.; Collaboration, I. Shift of Ag Diffusion Profiles in CdTe by Metal/Semiconductor Interfaces. *Appl. Phys. Lett.* **2012**, *100*, 171915.

(7) Franc, J.; Dědič, V.; Sellin, P. J.; Grill, R.; Veeramani, P. Radiation Induced Control of Electric Field in Au/CdTe/In Structures. *Appl. Phys. Lett.* **2011**, *98*, 232115.

(8) Qin, K.; Wang, L.; Zhang, J.; Min, J.; Huang, J.; Liang, X.; Tang, K.; Xia, Y. A Two-step Deposition Process for Electrode Fabrication of CdZnTe Detectors. *Vacuum* **2012**, *86*, 827−829.

(9) Yim, M. J.; Paik, K. W. Recent Advances on Anisotropic Conductive Adhesives (ACAs) for Flat Panel Displays and Semiconductor Packaging Applications. *Int. J. Adhes. Adhes.* **2006**, *26*, 304−313.

(10) Schlesinger, T. E.; Toney, J. E.; Yoon, H.; Lee, E. Y.; Brunett, B. A.; Franks, L.; James, R. B. Cadmium Zinc Telluride and Its Use as a nuclear Radiation Detector Material. *Mater. Sci. Eng., R* **2001**, *32*, 103−189.

(11) Zha, G.; Jie, W.; Bai, X.; Wang, T.; Fu, L.; Zhang, W.; Zhu, J.; Xu, F. The Study on the Work Function of CdZnTe with Different Surface States by Synchrotron Radiation Photoemission Spectroscopy. *J. Appl. Phys.* **2009**, *106*, 053714.

(12) Kalaitzakis, F. G.; Konstantinidis, G.; Sygellou, L.; Kennou, S.; Ladas, S.; Pelekanos, N. T. Effect of Boiling Aqua Regia on MOCVD and MBE p-type GaN Surfaces and Cr/p-GaN Interfaces. *Microelectron. Eng.* **2012**, *90*, 115−117.

(13) Bai, X.; Jie, W.; Zha, G.; Zhang, W.; Zhu, J.; Wang, T.; Yuan, Y.; Du, Y.; Wang, Y.; Fu, L. Interface Dipole and Schottky Barrier Formation at Au/CdZnTe(111)A Interfaces. *J. Phys. Chem. C* **2010**, *114*, 16426−16429.

(14) Qin, K.; Wang, L.; Min, J.; Zhang, J.; Huang, J.; Liang, X.; Tang, K.; Xia, Y. Effects of Contact Interface Degradation on the Performance of CdZnTe Detectors. *Vacuum* **2012**, *86*, 943−945.

(15) Kalaitzakis, F. G.; Pelekanos, N. T.; Prystawko, P.; Leszczynski, M.; Konstantinidis, G. Low Resistance As-deposited Cr/Au Contacts on p-type GaN. *Appl. Phys. Lett.* **2007**, *91*, 261103.

(16) Takahashi, K.; Tokudomi, S.; Nagata, Y.; Azuma, J.; Kamada, M. Surface Photo-voltage Effect on Cr/GaAs(100) Studied by Photo-emission Spectroscopy with the Combination of Synchrotron Radiation and Laser. *J. Appl. Phys.* **2011**, *110*, 11371.
(17) Tu, S. H.; Lan, C. J.; Wang, S. H.; Lee, M. L.; Chang, K. H.; Lin, R. M.; Chang, J. Y.; Sheu, J. K. InGaN Gallium Nitride liLght-emitting Diodes with Reflective Electrode Pads and Textured Gallium-doped ZnO Contact Layer. *Appl. Phys. Lett.* **2010**, *96*, 133504.
(18) Lee, M.-L.; Sheu, J.-K.; Hu, C. C. Nonalloyed Cr/Au-based Ohmic Contacts to n-GaN. *Appl. Phys. Lett.* **2007**, *91*, 182106.
(19) Tung, R. T. Recent Advances in Schottky Barrier Concepts. *Mater. Sci. Eng., R* **2001**, *35*, 1−138.
(20) Tung, R. T. Electron Transport at Metal-semiconductor Interfaces: General Theory. *Phys. Rev. B* **1992**, *45*, 13509−13523.
(21) Brillson, L. J. The Structure and Properties of Metal-semiconductor Interfaces. *Surf. Sci. Rep.* **1982**, *2*, 123−326.
(22) Perkowitz, S.; Kim, L. S.; Becla, P. Infrared Bond Ionicity in Ternary II−VI Alloys. *Solid State Commun.* **1991**, *77*, 471−474.
(23) Brillson, L. J. Chemical and Electronic Structure of Compound Semiconductor-metal Interfaces. *J. Vac. Sci. Technol.* **1982**, *20*, 652−658.
(24) Li, G.; Jie, W.; Wang, T.; Yang, G. Impurities in CdZnTe Crystal Grown by Vertical Bridgman Method. *Nucl. Instrum. Methods Phys. Res., Sect. A* **2004**, *534*, 511−517.
(25) Chastain, J.; Moulder, J. F.; King, R. C. Handbook of X-ray Photoelectron Spectroscopy: a Reference Book of Standard Spectra for Identification and Interpretation of XPS Data; Physical Electronics Division, Perkin-Elmer Corporation, U.S.: Chanhassen, MN, 1995.
(26) Peterman, D. J.; Franciosi, A. HgCdTe-Cr Interface Chemistry. *Appl. Phys. Lett.* **1984**, *45*, 1305.
(27) Franciosi, A.; Philip, P.; Peterman, D. Interface Chemistry of Ternary Semiconductors: Local Morphology of the $Hg_{1-x}Cd_xTe(110)$-Cr Interface. *Phys. Rev. B* **1985**, *32*, 8100−8107.
(28) Dharmadasa, I. M.; Patterson, M. H.; Williams, R. H. Chemical Reactions and Schottky Barrier Formation at Cr/n-CdTe Interfaces. *Semicond. Sci. Technol.* **1988**, *3*, 926.
(29) Trafas, B.; Hill, D.; Benning, P.; Waddill, G.; Yang, Y. N.; Siefert, R.; Weaver, J. Clustering and Reaction for Cr/GaAs(110): Scanning Tunneling Microscopy and Photoemission Studies. *Phys. Rev. B* **1991**, *43*, 7174−7184.
(30) Hölzl, J. Schulte, F. K., *Work Function of Metals*; Springer Berlin Heidelberg: Berlin, Germany, 1979.
(31) Michaelson, H. B. The work function of the elements and its periodicity. *J. Appl. Phys.* **1977**, *48*, 4729−4733.
(32) Tung, R. T. Chemical Bonding and Fermi Level Pinning at Metal-Semiconductor Interfaces. *Phys. Rev. Lett.* **2000**, *84*, 6078−6081.
(33) Vaynzof, Y.; Dennes, T. J.; Schwartz, J.; Kahn, A. Enhancement of Electron Injection into a Light-emitting Polymer from an Aluminum Oxide Cathode Modified by a Self-assembled Monolayer. *Appl. Phys. Lett.* **2008**, *93*, 103305.
(34) Otálvaro, D.; Veening, T.; Brocks, G. Self-Assembled Monolayer Induced Au(111) and Ag(111) Reconstructions: Work Functions and Interface Dipole Formation. *J. Phys. Chem. C* **2012**, *116*, 7826−7837.
(35) Bai, X.; Jie, W.; Zha, G.; Zhang, W.; Zhu, J.; Wang, T.; Yuan, Y.; Wang, Y.; Hua, H.; Fu, L. Adsorption of Water Molecules on the CdZnTe (111) B Surface. *Chem. Phys. Lett.* **2010**, *489*, 103−106.